

# Functional response regression with funBART: an analysis of patient-specific stillbirth risk

Jennifer E. Starling\*, Jared S. Murray, Carlos M. Carvalho,  
Radek Bukowski, and James G. Scott

May 20, 2022

## Abstract

This article introduces functional BART, a new approach for functional response regression—that is, estimating a functional mean response  $f(t)$  that depends upon a set of scalar covariates  $x$ . Functional BART, or funBART, is based on the successful Bayesian Additive Regression Trees (BART) model. The original BART model is an ensemble of regression trees; funBART extends this model to an ensemble of *functional* regression trees, in which the terminal nodes of each tree are parametrized by functions rather than scalar responses. Just like the original BART model, funBART offers an appealing combination of flexibility with user friendliness: it captures complex nonlinear relationships and interactions among the predictors, while eliminating many of the onerous “researcher degrees of freedom” involved in function-on-scalar regression using standard tools. In particular, functional BART does not require the user to specify a functional form or basis set for  $f(t)$ , to manually choose interactions, or to use a multi-step approach to select model terms or basis coefficients. Our model replaces all of these choices by a single smoothing parameter, which can either be chosen to reflect prior knowledge or tuned in a data-dependent way.

After demonstrating the performance of the method on a series of benchmarking experiments, we then apply funBART to our motivating example: pregnancy-outcomes data from the National Center for Health Statistics. Here, the goal is to build a model for stillbirth risk as a function of gestational age ( $t$ ), based on maternal and fetal risk factors ( $x$ ). We show how these patient-specific estimates of stillbirth risk can be used to inform clinical management of high-risk pregnancies, with the aim of reducing the risk of perinatal mortality.

The R package **funbart** implements all methods described in this article, and supplementary materials are available online.

**Keywords and phrases:** Bayesian additive regression trees (BART), ensemble methods, functional response regression, Gaussian processes, regression trees

---

\*Corresponding author: [jstarling@utexas.edu](mailto:jstarling@utexas.edu)

# 1 Introduction

## 1.1 Functional response regression

This paper proposes a new approach to the problem of functional-response regression, where we observe functional data  $y_i(t) = f(t; x_i) + e_i(t)$ , and where the goal is to estimate how the mean-response function  $f(t; x)$  depends upon a set of scalar predictors  $x = (x_1, \dots, x_p)$ . Our approach is called functional BART, or funBART, because it is based on the highly successful Bayesian Additive Regression Trees (BART) model introduced by Chipman et al. (2010).

The original BART model is a Bayesian ensemble-of-trees approach to nonparametric regression. It predicts a scalar response  $y$  using a sum of many binary regression trees, where each tree is encouraged by a prior to be a “weak learner”—that is, to have relatively few splits and to use only a small set of the available predictors. (Chipman et. al. refer to this as “shrinking toward additivity.”) Functional BART is similar in this regard; in fact, we use the same prior over tree space proposed in the original BART paper. Where funBART differs is in the prior used for the terminal nodes of each tree. BART is a model for a scalar response, and as such, it specifies a Gaussian prior for the (scalar) mean parameter in each terminal node. Functional BART, on the other hand, is a model for a *functional* response. We therefore replace the Gaussian prior with a prior over function space, so that each terminal node is parametrized by a function of  $t$ . The examples in this paper all use Gaussian-process priors for their flexibility and convenience, but in principle any prior over functions could be used.

As we will show, funBART is capable of modeling complex nonlinear relationships and interactions among the predictors, while still yielding smooth function estimates. At the same time, it eliminates many of the burdensome choices involved in standard approaches to function-on-scalar regression—for example, the need to manually specify interactions, or the need to select basis elements (e.g. spline knots) to regularize  $f(t; x)$ .

## 1.2 Motivating example: quantifying the risk of stillbirth

Our motivating example is from obstetrics, where one of the primary research goals is to quantify the risks of adverse pregnancy outcomes, and to provide clinicians with better knowledge and tools for managing those risks. In particular, we use funBART to analyze data on stillbirth, defined as fetal death after 20 weeks' gestation. Stillbirth is a major public-health problem, with 23,000 reported cases of stillbirth in the U.S. in 2013 alone (MacDorman and Gregory, 2015). Stillbirth is less well understood than other adverse pregnancy outcomes, and stillbirth rates have remained stubbornly level, even as other serious adverse perinatal outcomes (e.g. neonatal death) have become rarer. Providing better estimates of stillbirth risk as a function of gestational age can yield important insights for obstetricians and patients. In particular, if an obstetrician knew that a patient's stillbirth risk was likely to rise earlier in pregnancy than usual, or was likely to rise to higher than normal levels at specific gestational ages, then proactive steps could be taken to manage that risk. Conservative steps might entail increased monitoring and more frequent prenatal clinic visits, while a more aggressive step might involve an elective Caesarean section or the early induction of labor.

The key statistical point is that estimating stillbirth risk is a classic problem in functional response regression:

- We have a vector of predictors  $x$  representing characteristics of the maternal-fetal dyad—including maternal risk factors, such as diabetes, hypertension, and sociodemographic variables; and fetal characteristics, such as sex or ultrasound-estimated fetal weight).
- We want to understand how these predictors change the stillbirth hazard function  $h(t; x)$ , which represents the conditional probability of stillbirth at gestational age  $t$ , given that a fetus has survived in utero until just before  $t$ .

Unfortunately, the current literature in obstetrics does not provide an especially nu-

anced characterization of this hazard function. In particular, the way  $h(t; x)$  depends upon the predictors is not well understood. Perhaps the best evidence was compiled by Mandujano et al. (2013), who stratified patients into “high risk” and “low risk” categories based on the presence of at least one maternal condition from a long list (including diabetes, hypertension, and several others). This yields separate stillbirth risk-curve estimates for the high-risk and low-risk groups, but it does not meaningfully distinguish among the individual risk factors. Moreover, this approach does not incorporate recent findings that many other maternal and fetal characteristics—including maternal race, plurality, and sex of the fetus—appear to have some relationship with risk of stillbirth (Xu et al., 2013).

To address this evidentiary gap, we apply funBART to estimate patient-specific stillbirth risk functions using data on publicly available pregnancy records from the National Center for Health Statistics. Our analysis provides obstetricians with new evidence to evaluate each patient’s individual risk of stillbirth, potentially giving them tools to improve the advice they give their patients about how to minimize the risk of perinatal mortality.

It would certainly be possible to apply existing techniques for functional regression in an attempt to accomplish the same goal. As we will show, however, doing so would be far from straightforward. In particular, existing techniques do not make it easy to model  $h(t; x)$  in a way that incorporates complicated interactions and nonlinear effects of the maternal-fetal covariates  $x$ , while maintaining computational tractability and providing a full picture of uncertainty. Yet the stillbirth-risk estimation problem imposes all of these requirements; to cite one example of a clinically plausible interaction, the increase in risk from having both diabetes and hypertension might be greater than the combined increase from having either factor alone. Functional BART is designed with these kinds of interactions and nonlinearities in mind; indeed, our analysis reveals support for precisely this finding of a diabetes/hypertension interaction (see Section 5). Yet despite being

so flexible, funBART simultaneously minimizes the “researcher degrees of freedom” that typically arise in fitting a complicated functional regression model, including the choice of functional form, the selection/regularization of basis elements, and the manual specification of interactions.

### 1.3 Outline

The rest of the article proceeds as follows. Section 2 presents the functional BART model and reviews the relevant literature. Section 3 describes how to fit the functional BART model by extending the Bayesian Backfitting algorithm by Chipman et al, and offers suggestions for hyperparameter selection. Section 4 presents results of a simulation study that validates funBART’s performance. Section 5 provides background information on the stillbirth risk-curve modeling problem and presents analysis and results. Section 6 contains discussion.

All methods described in this paper are implemented in the R package **funbart**.<sup>1</sup>

## 2 The functional BART model

### 2.1 The BART model

Before introducing our functional BART model, we briefly review the original BART framework. BART, which stands for Bayesian Additive Regression Trees, is a fully Bayesian ensemble-of-trees model (Chipman et al., 2010). BART models the mean response for a non-linear regression function as the sum of a large number of binary trees, each of which is constrained by the BART prior to be quite shallow (and therefore a weak learner). The model is defined by a likelihood and prior, and inference is performed by sampling from the posterior. Let  $y_i$  be a scalar response and  $x_i$  be a vector of covariates. The BART model

---

<sup>1</sup><https://github.com/jestarling/funbart>

assumes that

$$y_i = f(x_i) + \epsilon_i, \quad \epsilon_i \stackrel{iid}{\sim} N(0, \sigma^2) \quad (1)$$

$$f(x_i) = \sum_{j=1}^m g(x_i; T_j, M_j). \quad (2)$$

Here each  $T_j$  is a binary tree that induces a step function in  $x$  via a partition of the covariate space, while the  $M_j = \{\mu_{1j}, \dots, \mu_{bj,j}\}$  are the  $b_j$  terminal node values in tree  $j$  (i.e. the levels of the step function). We can think of each  $g$  as a basis function parameterized by the binary tree defined by  $(T_j, M_j)$ .

The BART prior consists of three elements. The first component is the conjugate prior for the error variance,  $\sigma^2 \sim \nu \lambda / \chi_\nu^2$ . The second component is the specification of independent Gaussians  $\mu_{hj} \stackrel{iid}{\sim} N(\mu_0, \tau^2)$  on the terminal node parameters  $M_j = \{\mu_{1j}, \dots, \mu_{bj,j}\}$  of each tree. The third component is the prior over tree space, composed of a set of probabilities governing three things: the choice of splitting covariate, the choice of splitting value for each covariate, and whether a node at a given depth is a terminal node. We refer interested readers to Chipman et al. (2010), who recommend default hyperparameters that favor shallow trees, which both regularizes the estimate and encourages rapid mixing.

Chipman et al. also provides a probit version of the BART model for binary outcomes, where:

$$p(Y = 1 \mid x) = \Phi(G(x)), \text{ where} \quad (3)$$

$$G(x) = \sum_{j=1}^m g(x; T_j, M_j) \quad (4)$$

where  $\Phi(\cdot)$  is the standard normal CDF. Inference proceeds via data augmentation, in the manner of Albert and Chib (1993). Our functional BART can be extended in precisely the same way, as we illustrate below.

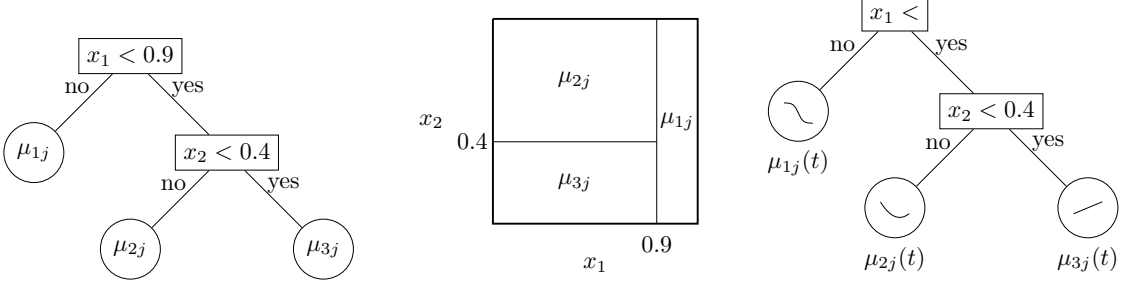


Figure 1: (Left) An example binary tree  $T_j$  where terminal nodes are labeled with the corresponding scalar parameters  $\mu_{hj}$ . (Middle) The corresponding partition of the sample space and the step function  $g(T_j, M_j)$ . (Right) Our functional BART modification, where the  $\mu_{hj}(t)$  parameters associated to terminal nodes are now functions of time.

## 2.2 Functional BART

Now consider a functional response regression problem,  $y_i(t) = f(t; x_i) + \epsilon_i(t)$ , where the underlying mean function  $f(t; x_i)$  depends on a set of scalar covariates  $x_i$ . To adapt the BART model to this domain, we replace the scalar node-level parameters  $\mu_{hj}$  in with univariate functions in  $t$ ,  $\mu_{hj}(t)$ . (See Figure 1.) These univariate functions can in principle be assigned any prior over function space; in the applications considered in this paper, we use Gaussian process priors.

More formally, we express the functional BART model as follows. Suppose that each observation  $i$  in our data set consists of a predictor variable  $x_i$  together with pairs  $(y_{ik}, t_{ik})$  for  $k = 1, \dots, N_i$ , where  $y_{ik}$  is the measured response at  $t_{ik}$ . (Colloquially we refer to  $t$  as time, although in principle it can index any metric space.) Letting  $e_i = (e_1, \dots, e_{N_i})^T$  represent a vector of residuals, we assume that

$$y_i(t) = \alpha(t) + f(t; x_i) + \epsilon_i(t), \quad \epsilon_i \sim N(0, \Sigma_i) \quad (5)$$

$$f(t; x_i) = \sum_{j=1}^m g_j(t, x_i; T_j, M_j). \quad (6)$$

Here  $T_j$  is a binary tree whose terminal nodes partition the covariate space into  $b_j$  disjoint regions, just as in the original BART model; while  $M_j = \{\mu_{1,j}(t), \dots, \mu_{b_{j,j}}(t)\}$ , with each  $\mu_{h,j}(t)$  associated with one terminal node. The right panel of Figure 1 illustrates an

example where  $b_j = 3$ .

We use the same prior over tree space as in the original BART paper. To model the  $\mu_{hj}(t)$ 's in each terminal node, we use a zero-centered Gaussian process prior:

$$\mu(t) \sim GP(0, C_\theta(t, t')) ,$$

where  $C_\theta(t, t')$  is the covariance function with hyperparameter  $\theta$ , which can be either chosen based on prior knowledge or tuned using the data. (Zero-centering is appropriate here because we separate out the mean term  $\alpha(t)$  in Equation 5.)

In principle any covariance function can be used. For all examples in this paper, we use the squared-exponential covariance function with variance parameter  $\tau^2/m$  and length scale  $l$ . That is,

$$C(t, t') = \frac{\tau^2}{m} \exp \left\{ -\frac{d(t, t')^2}{2l^2} \right\} , \quad (7)$$

where  $d(t, t')$  is the Euclidean distance between  $t$  and  $t'$ . Here  $\tau^2$  determines the marginal variance of the  $\mu_{hj}$ 's, while  $l$  governs their “wigginess.” As in the original BART model, we scale the variance parameter  $\tau^2$  inversely by the number of trees  $m$ . Since the mean-response function  $f(t; x)$  is the sum of  $m$  trees, this implies that the marginal variance of  $f(t; x)$  at any point  $t$  is  $\tau^2$ . We then assign  $\tau$  a half-Cauchy prior,  $\tau \sim C^+(0, 1)$ , as in Gelman (2006) and Hahn et al. (2017).

The funBart model also requires specifying  $l$ , the length scale of the Gaussian process prior. This length scale can be set using prior knowledge, but in Section 3.3 we provide a method to tune it automatically over a grid of possible values. As we also explain in Section 3.3, a reasonable default choice when using the squared exponential covariance function is  $l = T/\pi$ , where  $T$  is the range of  $t_{ik}$  values in the data set.

The final parameter to specify is  $\Sigma_i$ , the covariance matrix of the  $i$ th vector of residuals  $(e_{i1}, \dots, e_{iN_i})^T$ . The appropriate structure of  $\Sigma_i$  will be context-dependent. In all examples in this paper, we assume an *i.i.d* error structure in which  $\Sigma_i = \sigma^2 I_{N_i}$ , where  $I_{N_i}$  is the

identity matrix of appropriate dimension. We then complete the model specification by assigning  $\sigma^2$  an inverse chi-square distribution  $\sigma^2 \sim \nu\lambda/\chi_\nu^2$ .

## 2.3 Connection with existing work

We first present a brief review of functional response regression, followed by discussion of literature related to BART and our functional BART extension. For more general reviews of functional regression, we refer the interested reader to Ramsay (1997) and Morris (2014).

**Functional response regression.** Most existing work on functional-response regression, also called function-on-scalar regression, is based on the functional linear model:

$$y_i(t) = \alpha(t) + \sum_{j=1}^p x_{ij}\beta_j(t) + e_i(t),$$

where the functional coefficient  $\beta_j(t)$  represents the partial relationship between the mean response and predictor  $x_i$  at location  $t$ . But the functional linear model raises several challenges, especially in the context of the stillbirth prediction problem. How should  $\beta_j(t)$  be represented and regularized? What if the effect of  $x_j$  is nonlinear? And how should interactions among the predictors be incorporated?

Consider first the question of how to represent  $\beta_j(t)$ , which is typically done via an expansion in a user-chosen basis. Morris (2014) notes that splines are well suited to smooth functions in settings with a low-dimensional grid, while Fourier polynomials are more suited to stationary periodic functions. Wavelets handle discontinuities, spikes, and non-stationary features, while a principal-component basis tends to perform well when there is long-range between-function correlation. Regularization is achieved in different ways depending on the method. For a spline basis, regularization is often accomplished by specifying relatively few knots—although this raises the question of exactly how many

knots should be chosen. Other common choices involve enforcing sparsity via L1 regularization, penalizing roughness via L2 regularization, and hard thresholding of basis coefficients. Other, more complex approaches to regularization have also been studied; for example, Shi et al. (2007) propose a multi-step modeling approach incorporating B-splines followed by Gaussian processes. Eilers and Marx (1996) propose addressing difficulty of number and position of knots using a large number of knots with a difference penalty on coefficients of adjacent B-splines. Ramsay (1997) proposed separate point-wise regressions for each  $t$ , and discussed regularization using roughness penalties and basis functions.

In our functional BART model, on the other hand, regularization is governed by a single smoothing parameter  $l$ , the length scale of the underlying Gaussian process prior. This parameter is easily tuned by cross validation or using information criteria (e.g. WAIC); moreover, we have found that the default choice  $l = T/\pi$  works well across a broad range of settings.

Another difficult challenge in the functional linear model is handling nonlinearities and interactions among the covariates. Nonlinearities in some numerical predictor  $x_j$  can, in principle, be addressed by expanding  $x_j$  in its own basis (e.g. splines) and adding a functional coefficient to the model for every basis element in  $x_j$ . Similarly, two-way linear interactions can, in principle, be addressed by adding a product of the form  $x_{ij}x_{ik}\beta_{jk}(t)$  to the functional linear model, and estimating the interaction term  $\beta_{jk}(t)$ . This may be a satisfactory approach if data is abundant and the right pattern of interactions is known with certainty beforehand. But if the right pattern of interactions is unknown or is suspected to be nonlinear, then the standard “outer-product basis” strategy results in a potentially explosive number of interactions among individual basis elements for  $x_j$ ,  $x_k$ , and  $\beta_{jk}(t)$ . For example, if  $x_j$ ,  $x_k$  and  $\beta_{jk}(t)$  are each represented using a spline basis with 7 degrees of freedom, then including a nonlinear two-way interaction between  $x_j$  and  $x_k$  requires estimating  $7^3 = 343$  individual coefficients. This poses an extremely challenging bias-

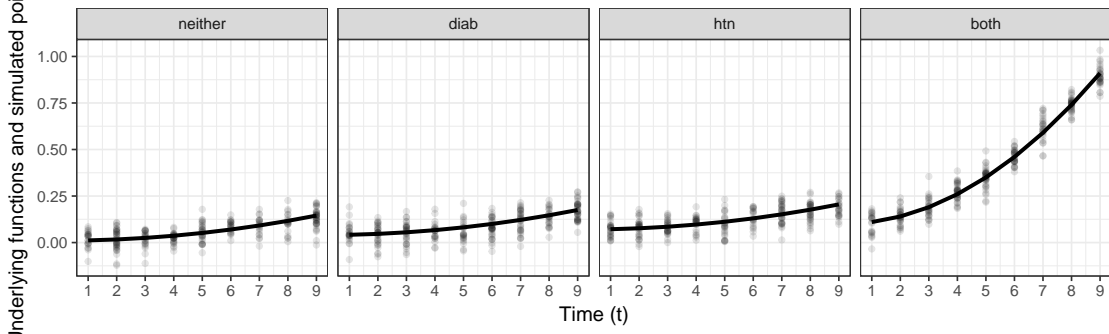


Figure 2: Simulated data for spline comparison.

variance tradeoff.

**A toy example** Difficulties with nonlinearities and interactions also aBayesian backfitting (scalar) regression, but they are much more severe in functional response regression. In practice, the need to select and regularize interaction terms results in a potentially large specification search for the right functional form of the model, opening the door to many of the more pernicious forms of “data snooping,” “p-hacking,” and the “garden of forking paths,” as noted by e.g. Hill (2011) in the context of causal inference. Functional BART, on the other hand, is capable of finding multiway interactions while avoiding the specification search entirely.

To illustrate these points, we now show the performance of funBART on a toy example that is intended to resemble a highly stylized version of the stillbirth-prediction problem we consider in Section 5. In particular, the example is characterized by a strong interaction between two binary covariates, representing diabetes and hypertension. We simulated  $n = 1000$  observations at randomly selected time points  $t_i \in \{1, \dots, 9\}$ , representing gestational age of pregnancy. We then generate two binary covariates  $x_i = (d_i, h_i)$  for each subject, where  $d_i$  is an indicator for presence of diabetes and  $h_i$  is an indicator for presence of hypertension. The underlying functional-response model is

$$f(t; x_i) = \left[ \frac{t^2}{6 - 5h_i d_i} + 1 + 3d_i + 6h_i \right] / 100.$$

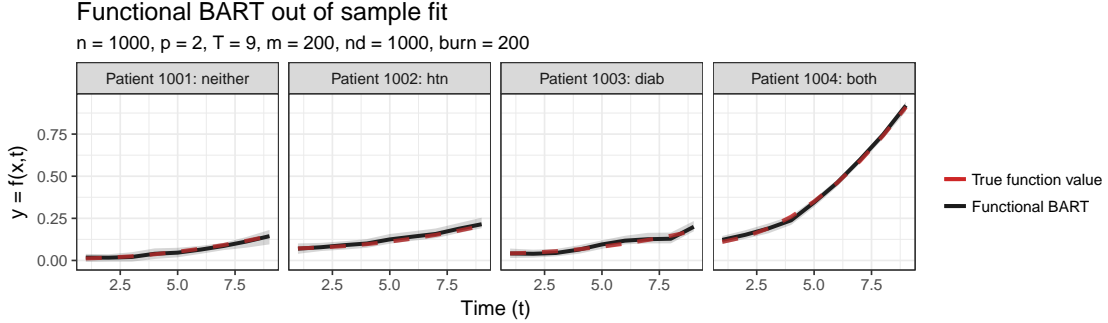


Figure 3: Simulated data for spline comparison.

This yields four different functional mean responses, one for each combination of diabetes and hypertensive status (Figure 2). Diabetes ( $d_i$ ) and hypertension ( $h_i$ ) each have small main effects, and together they have a large interaction that affects the risk of stillbirth primarily at later gestational ages.

We first fit the data using the functional BART model, using 200 trees, 200 burn-in iterations, and 1000 iterations of the MCMC. We tune the length-scale parameter using the method described in the Appendix. Figure 3 illustrates the predicted fits and posterior credible intervals for observations with each of the four combinations of presence or absence of diabetes and hypertension. The model easily discovers the two-way interaction, without inflating the variance in other parts of the predictor space.

We then fit four spline models (Figure 4). We choose B-spline basis functions, and begin with cubic splines using 7 degrees of freedom. The first row of the panel gives out-of-sample fits for the spline model with no interaction term, and these fits are predictably poor given the strong interaction between diabetes and hypertension. The second row of the panel adds a linear interaction term between hypertension and diabetes, again yielding fairly poor fits, especially in the case where both diabetes and hypertension are present. The third row of the panel illustrates the dangers of overfitting in spline models. The model has a full interaction between the basis splines, diabetes, and hypertension, yielding good out of sample fit for the diabetes-and-hypertension case, but poor fits in the other three cases. The fourth row of the panel keeps the full spline interaction and

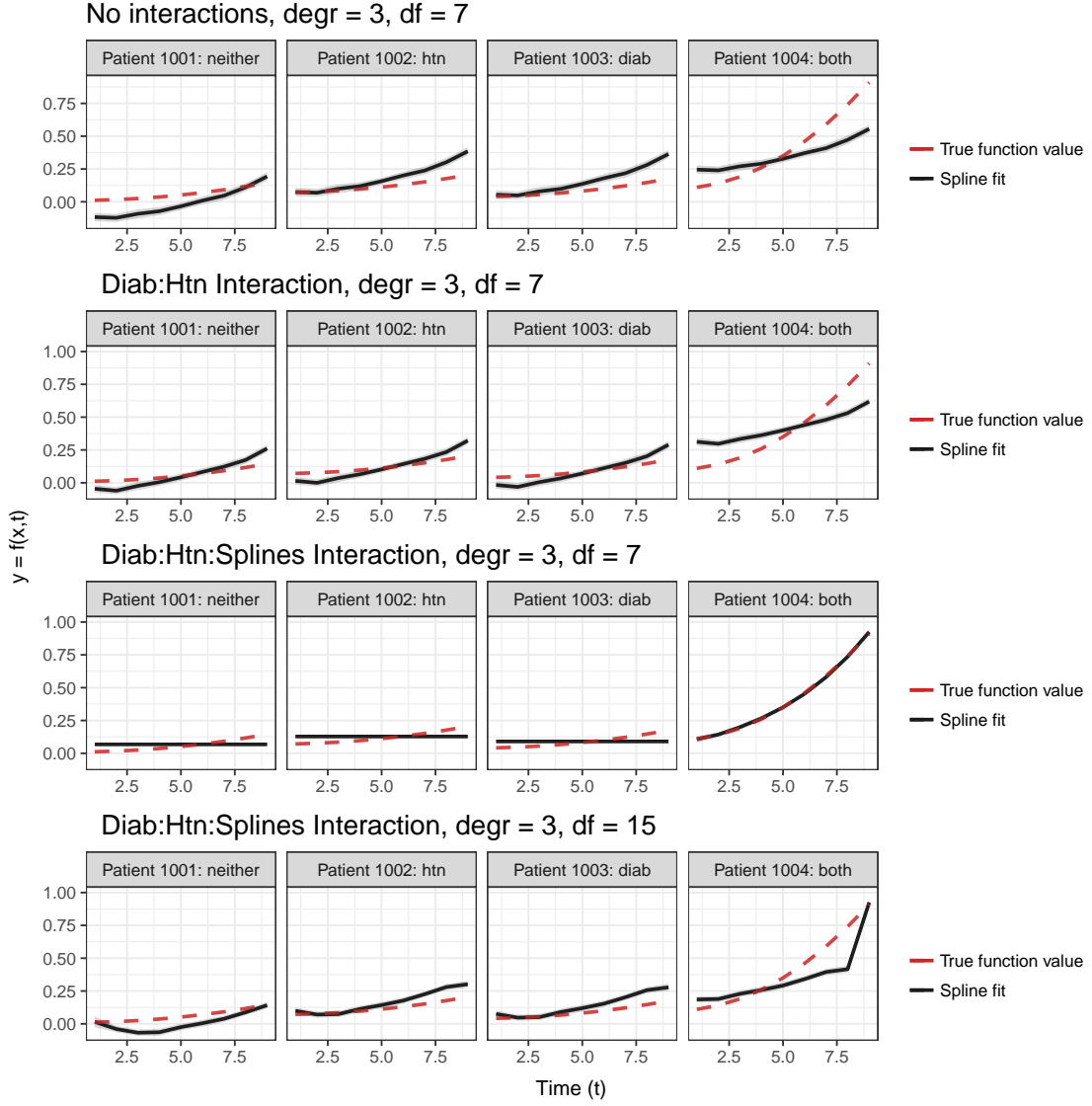


Figure 4: Spline fits panel

increases degrees of freedom to 15. The resulting fit is quite erratic. Functional BART outperforms in each of the four scenarios.

We do not intend to imply that Figure 4 represents the best fit one could expect in this scenario using the functional linear model with a spline basis. It would surely possible to do better here, perhaps by dynamically selecting knot locations, or by introducing many more basis elements and then regularizing the coefficients. Our point is simply that all of these steps all involve a series of subjective choices, as well as considerable further effort by the data analyst—and that this effort becomes substantially harder with more

variables, more interactions, multi-way interactions, or numerical predictors that have nonlinear effects on the functional mean response.

With functional BART, on the other hand, we do not need to specify either a basis set or a set of interactions. We get excellent results out of the box using default parameter settings, with no user-specified inputs.

**Existing work on Bayesian tree models.** Our paper sits in a long line of other research on extensions to the Bayesian tree-modeling framework. Two papers in particular are especially close in spirit to ours. The first is the treed Gaussian process model of Gramacy and Lee (2008). Their model represents a functional response using a single deep tree with a Gaussian process in each terminal node. Our model, on the other hand, is a sum of many trees. Our work therefore generalizes that of Gramacy and Lee (2008) in the same way that the BART model generalizes the single-tree Bayesian CART model of Chipman et al. (1998).

The second is Sparapani et al. (2016), who introduce a model for nonparametric survival analysis using BART. This model incorporates dependence on  $t$  by simply adding it as a covariate to an ordinary BART model for scalar regression. Thus it is not a true functional-response regression model, and it is incapable of imposing any continuity or smoothness constraints on  $f(t; x)$ . In Section 4, we will show that this lack of smoothness results in suboptimal estimates.

All of the other research on BART concerns the problem of ordinary scalar regression, and we highlight some select recent works here. Linero and Yang (2017) present a formulation of the BART model which induces smoothness across all covariates by effectively replacing the step function induced by the binary trees with sigmoids. Kapelner and Bleich (2014) modify the BART framework to incorporate missingness into the structure of decision trees by incorporating missingness into the splitting rules for each tree. Hill (2011) presents a framework for using BART to model the response surface and es-

timate causal effects, including heterogenous treatment effects. Hahn et al. (2017) extend this framework to address the treatment bias introduced by regularization-induced confounding.

Computational efficiency of the BART model for large data sets and high-dimensional predictors is also a notable concern and an active area of research. Pratola et al. (2014) scales BART for large data sets by considering only a subset of the proposed tree moves (prune and grow). Lakshminarayanan et al. (2015) present a Particle Gibbs sampler which proposes full tree samples instead of local moves to encourage faster mixing. Linero (2018) address high-dimensional data with a modification to the tree prior which induces sparsity via a Dirichlet hyperprior on the splitting proportions. Hernández et al. (2018) propose a modified BART model, BART-BMA, which uses Bayesian model averaging and a greedy search algorithm to obtain the posterior efficiently in the high-dimensional case.

Additional work addresses applications of BART in the variable selection case. We do not comprehensively review this literature, but we do note the contribution of Bleich et al. (2014), who apply BART for variable selection in gene regulation and include the open source R package **bartMachine** (Kapelner and Bleich, 2014). We provide the open source R package **funbart** to implement our work, and we have benefited from a rich selection of existing BART software implementations, including **bartMachine**, as well as **BART** (McCulloch et al., 2018), **BayesTrees** (Chipman and McCulloch, 2016) and **fastbart** (Hahn et al., 2017).

## 3 Fitting the functional BART model

### 3.1 Bayesian backfitting MCMC

The original BART model is typically fit using an algorithm that Chipman et al. called Bayesian Backfitting. We first review this algorithm, before describing the modifications necessary to fit the functional BART model.

Bayesian Backfitting involves sampling each tree and its parameters one at a time, given the partial residuals from all other  $m - 1$  trees. One iteration of the sampler consists of looping through the  $m$  trees, sampling each tree  $T_j$  via a Metropolis step, and then sampling its associated leaf parameters  $M_j$ , conditional on  $\sigma^2$  and the remaining trees and leaf parameters. After a pass through all  $m$  trees,  $\sigma^2$  is updated in a Gibbs step.

To sample  $\{T_j, M_j\}$  conditioned on the other trees and leaf parameters  $\{T_{(j)}, M_{(j)}\}$ , define the partial residual as

$$R_{ij} = y_i - \sum_{k=1, k \neq j}^m g(x_i; T_k, M_k). \quad (8)$$

Using  $R_j$  as the working response vector, at step  $s$  of the MCMC one samples  $T_j^{(s)}$  by proposing one of four local changes to  $T_j^{(s-1)}$ , marginalizing analytically over  $M_j$ . The local change is selected randomly from the following candidates:

- **grow** randomly selects a terminal node and splits it into two child nodes
- **prune** randomly selects an internal node with two children and no grandchildren, and prunes the children, making the selected node a leaf
- **change** randomly selects an internal node and draws a new splitting rule
- **swap** randomly selects a parent-child pair of internal nodes and swaps their decision rules

The **change** and **swap** moves are computationally expensive; in practice, BART is often implemented with only **prune** and **grow** proposals. Once the move in tree space is either accepted or rejected,  $M_j$  is sampled from its Gaussian full conditional, given  $T_j$  and  $\sigma^2$ .

## 3.2 Modifications for functional BART

Our approach to fitting functional BART retains the form of the Bayesian Backfitting MCMC algorithm, as detailed by Chipman et al. (2010). The primary modification is that

all conjugate updates are modified to their multivariate forms. We assume an i.i.d. error structure, although this is easily modified; and we also use a redundant multiplication parameterization of the scale parameter, to facilitate faster MCMC mixing (Gelman, 2006; Hahn et al., 2017). Thus our model is

$$\begin{aligned}
y_i(t) &= \alpha(t) + \eta f(t; x_i) + \epsilon_i(t), \quad \epsilon_i(t) \stackrel{iid}{\sim} N(0, \Sigma_i) \\
f(t; x_i) &= \sum_{j=1}^m g_j(t, x_i; T_j, M_j), \quad M_j = \{\mu_{1,j}(t), \dots, \mu_{b_j,j}(t)\} \\
\mu_{hj}(t) &\sim \text{GP}(0, C(t, t')) \\
\eta &\sim N(0, \gamma^2) \\
\gamma &\sim IG(1/2, 1/2) \\
\sigma^2 &\sim \nu \lambda / \chi_\nu^2.
\end{aligned}$$

Recall that  $\mu_{hj}(t)$  is the function at terminal node  $l$  of tree  $j$ . As described previously, this function has a Gaussian process prior with squared exponential covariance function with length scale  $l$ . Because we have already introduced  $\eta$  as a leading multiplicative scale parameter, we set the variance parameter of the covariance function to be  $1/m$ .

We use the same prior for over trees  $T_j$  as in Chipman et al. (2010) and Hahn et al. (2017), and so we omit many details here and refer the interested reader there. Specifically, these papers parametrize tree depth in terms of the pair  $(\alpha, \beta)$ ; we set  $(\alpha = .95, \beta = 2)$ , which puts high probability on trees of depth 2 and 3, and minimizes probability on trees with depth 1 or greater than 4. For  $\sigma^2$ , we follow Chipman et al.'s recommendation for a rough over-estimation of  $\hat{\sigma}$ . We choose  $\nu = 3$  and  $q = 0.90$ , and estimate  $\hat{\sigma}$  by regressing  $y$  onto  $x$ , then choosing  $\lambda$  s.t. the  $q$ th quantile of the prior is located at  $\hat{\sigma}$ , i.e.  $P(\sigma \leq \hat{\sigma}) = q$ .

The posterior conditional distributions are as follows. For simplicity of notation, we assume times  $t_{ik}$  are on a discrete grid, where  $T$  is again the range of  $t_{ik}$  values in the data

set. We update  $\sigma^2$  as

$$(\sigma^2 | \dots) \sim \frac{\nu\lambda + RSS}{\chi_{\nu+N+1}^2} \quad \text{where } RSS = \sum_{i,t} (y_i(t) - \eta f(x_i, t))^2.$$

where  $N$  is the count of observations across all time points,  $N = \sum_{i=1}^n N_i$  where  $N_i$  is the number of time points for observation  $i$ , and  $\chi_{\nu+N+1}^2$  is a draw from a chi-squared random variable.

The update for each  $\mu_h = [\mu_h^{(1)}, \dots, \mu_h^{(T)}]$  is

$$(\mu_h | \dots) \sim N\left(\tilde{m}, \tilde{\Sigma}\right) \quad \text{where } \tilde{\Sigma} = (\Lambda + K)^{-1} \text{ and } \tilde{m} = \tilde{\Sigma}(\Lambda \bar{y}_l + K \mu_0)$$

where  $\Lambda = N_l^{-1}$  is the inverse of the diagonal matrix of sample sizes for each time point for observations in leaf  $l$ ,  $K = \Sigma_0^{-1}$ , and  $\bar{y}_l$  is the vector of sample means for observations in leaf  $l$  at each time point.

The update for  $\eta$  is Gaussian,

$$(\eta | \dots) \sim N(\tilde{m}, \tilde{v}^2) \quad \text{where } \tilde{v}^2 = \left( \frac{1}{\gamma^2} + \frac{1}{\sigma^2} \sum_{i,t} f(t; x_i)^2 \right)^{-1} \text{ and } \tilde{m} = \tilde{v}^2 \left( \frac{1}{\sigma^2} \sum_{i,t} y_i f(t; x_i) \right). \quad (9)$$

Finally, the update for  $\gamma^2$  is

$$(\gamma^2 | \dots) \sim \text{IG}\left(1, \frac{\eta^2 + 1}{2}\right).$$

For updating the trees  $T_j$ , the marginal likelihood is the corresponding multivariate extension to the marginal likelihood in vanilla BART. We again let  $R_{ij}$  represent the partial residuals as defined in Equation 8, and let  $R_l$  denote the vector containing residuals for

data points in leaf  $l$ . We then obtain the marginal likelihood for the  $b$  terminal nodes as

$$p(R_h \mid T_j, M_j, \sigma^2) = \int_{\mu_h} \prod_{l \in 1:b} N(R_h \mid W_l \mu_h, \sigma^2 I) \cdot N(\mu_h \mid \mu_0, \Sigma_0) \partial \mu_h$$

where  $W_l$  is a  $(T \times n)$  matrix where elements indicate times at which each  $y_{ik}$  is observed.

### 3.3 Tuning the length scale $l$

We must also select  $l$ , the length-scale parameter of the covariance matrix. To do this, we represent  $l$  using a formula by Kratz (2006) for the expected number of times a random function crosses its mean,  $E[N_T(s)]$ , on some interval  $I = [0, T]$ . This formula gives us a closed-form solution for the length-scale parameter as a function of the expected number of times that  $f(t; x)$  crosses zero. Recall that if  $f(t; x) = 0$ , then the overall functional response at predictor  $x$  is simply  $\alpha(t)$ , which we can think of as an the overall mean response function, or functional “intercept.”

We can think of the expected number of crossings as an intuitive measure for the wiggliness of our functional response. Let  $r(s)$  be the correlation function between time 0 and time  $s$ ,

$$r(s) = \frac{E[\{f(x, 0) - \mu(0)\} \{f(x, s) - \mu(s)\}]}{sd(f(x, 0)) \cdot sd(f(x, s))}.$$

Per Kratz,

$$E[N_T(s)] = T \cdot \exp\left[-\frac{s^2}{2}\right] \left(\frac{\sqrt{r''(0)}}{\pi}\right)$$

and we let  $s = 0$ . We use the squared exponential covariance kernel, so  $r(t) = \frac{Cov(f(x, 0), f(t; x))}{\tau^2} =$

$\exp\left[-\frac{t^2}{2l^2}\right]$ . Some algebra yields

$$l = \frac{T}{\pi E[N_T(0)]} \quad (10)$$

This opens up several options for choosing the length scale. The first is by subjective choice. This would entail eliciting a guess for  $\kappa \equiv E[N_T(0)]$ , the average number of times that  $f(x, t)$  will cross zero across all values of the covariate—or equivalently, the average number of times that each functional response  $\alpha(t) + f(x, t)$  will cross the overall mean response  $\alpha(t)$ . This is a useful basis for elicitation, since the number of crossings is a sensible and intuitive measure of wiggleness.

The second option is to choose a default value for  $\kappa$ . If a default must be chosen, we recommend  $\kappa = 1$ , or equivalently,  $l = T/\pi$ . This encodes the belief that each functional response will cross the overall mean response  $\alpha(t)$  once, on average across all predictor values. This allows for a substantial amount of heterogeneity in the functional mean responses, while still shrinking towards the overall mean.

A final option, which we use in our simulation studies and real-data examples, is to tune  $\kappa = E[N_T(0)]$  over a grid of candidate values. This could be done using cross validation, as in the original BART paper, although we use WAIC (Watanabe, 2013), because it provides an estimate of generalization error without requiring that we split the data into multiple subsets; see the Appendix for details. In our simulation, we note that values of  $\kappa \approx 1$  are frequently chosen by this data-driven approach, lending further credence to the choice of  $\kappa = 1$  as a reasonable default.

## 4 Simulations

### 4.1 Toy example using cosines

We simulate a data set with four covariates  $x_i = (x_{i1}, \dots, x_{i4})$ . Each pair of covariates are generated from a bivariate Gaussian with moderate correlation and unit variance. We use eight discrete time points ( $T = 8$ ) and sample size  $n = 500$ . We calculated the underlying function  $f(t; x)$  for each dataset as

$$f(x; t) = g(x_1, x_2) \cdot \cos(t + 2\pi h(x_3, x_4)) \quad (11)$$

so that varying covariate combinations modify both amplitude and phase shift. We let  $g$  and  $h$  be simple functions of the covariate pairs; here we sum each pair of covariates.

We fit the simulated dataset using both BART and functional BART, using 1000 draws after burning 200, with 200 trees.

### 4.2 Simulation study

This section presents the results of a simulation study that confirms the advantage of the functional BART model for estimating functional responses. The focus of our benchmarking is on comparing functional BART to ordinary BART in which we simply introduce  $t$  as another predictor to the model. This will illustrate the benefits of using a true functional regression model, as opposed to treating functional regression as a special case of scalar regression.

We simulated datasets with four covariates  $x_i = (x_{i1}, \dots, x_{i4})$ , eight covariates  $x_i = (x_{i1}, \dots, x_{i8})$ , and twenty covariates  $x_i = (x_{i1}, \dots, x_{i20})$ . We generate each pair of covariates  $(x_{ij}, x_{i,j+1})$  for odd  $j$  from a bivariate Gaussian with moderate correlation and unit variances. For all scenarios, we used eight discrete time points ( $T = 8$ ). For each number of covariates, we include sample sizes  $n \in \{100, 500, 1000, 2500\}$ , for a total of twelve con-

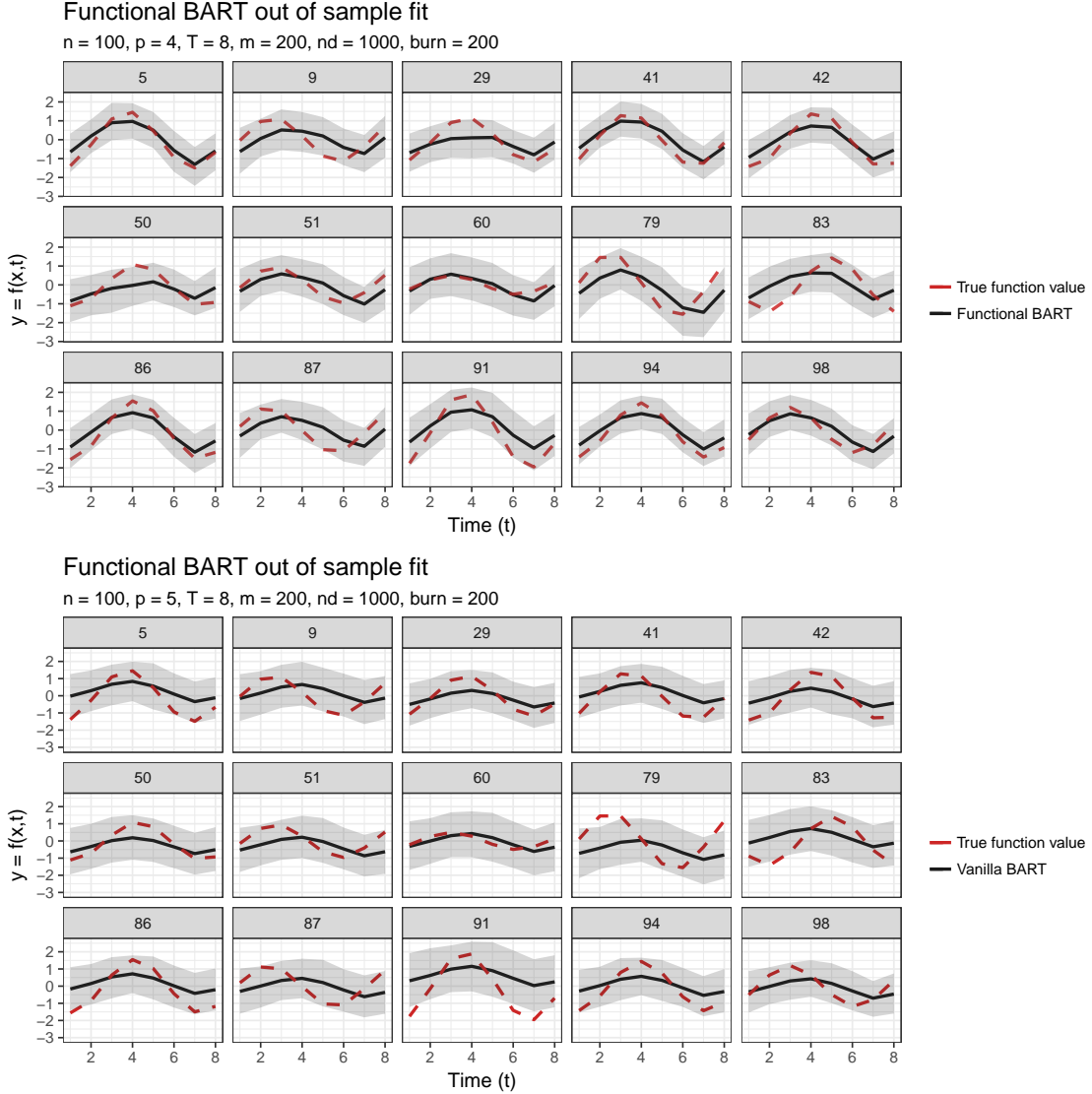


Figure 5: Toy example comparison of Functional BART and BART

figurations of sample size and dimension. For each of the twelve possible combinations of sample size and covariate dimension, we simulated 100 datasets.

In the  $p = 4$  case, the true mean functional response is

$$f(t; x) = g(x_1, x_2) \cdot \cos(t + 2\pi h(x_3, x_4)) \quad (12)$$

so that  $(x_1, x_2)$  modify the function's amplitude and  $(x_3, x_4)$  modify its phase. In the  $p = 8$

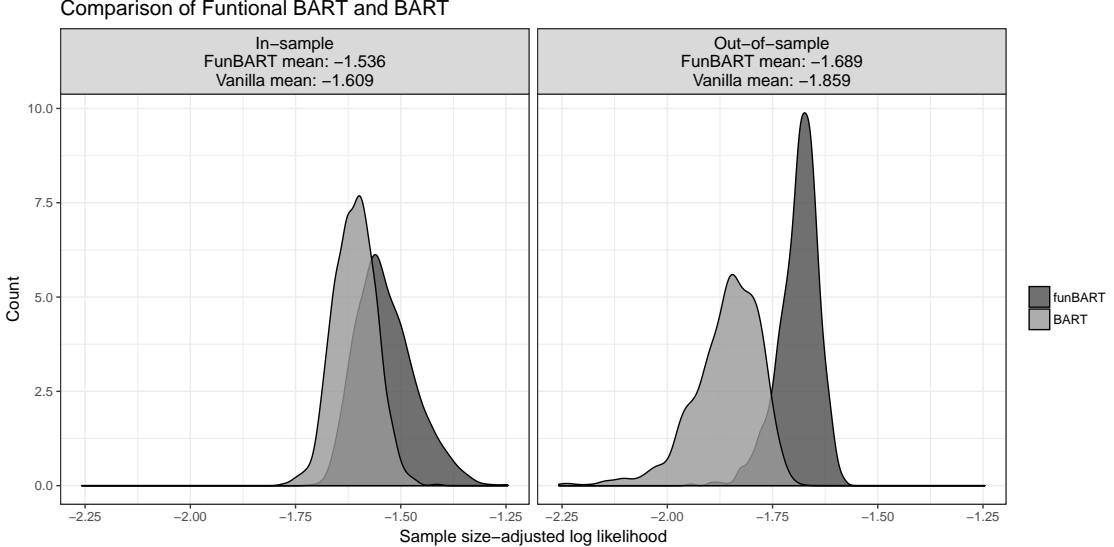


Figure 6: Log density comparison

and  $p = 20$  cases, we continue in similar fashion, alternating sines and cosines, so that

$$f(t; x) = g(x_1, x_2) \cdot \cos(t + 2\pi h(x_3, x_4)) + g(x_3, x_4) \cdot \sin(t + 2\pi h(x_5, x_6)) + \dots \quad (13)$$

where this pattern continues. We let  $g$  and  $h$  be simple functions of the covariate pairs; in particular, we sum each pair of covariates. We generate one time point per design point  $x_i$ , drawn uniformly from the vector of eight discrete time points.

We compare vanilla BART and functional BART using  $m = 200$  trees, 200 burn-in MCMC iterations, and 1000 iterations. We compare performance by calculating the log-likelihood at each iteration of the algorithm, both in-sample and for a held-out sample, and by taking the mean log-likelihood across all MCMC iterations. Log-likelihoods are scaled by sample size. We tune the length scale  $l$  using the method described in the Appendix.

In our scenarios, where the functional response evolves smoothly over time, functional BART consistently outperforms vanilla BART (Table 1) in out of sample log-likelihood. While the in-sample fits are reasonably close as measured by log likelihood, the out-of-sample fit is far better under the functional BART model.

p	n	In-sample		Out-of-sample	
		BART	FunBART	BART	FunBART
4	100	-1.61	<b>-1.49</b>	-1.97	<b>-1.92</b>
4	500	-1.53	<b>-1.47</b>	-1.8	<b>-1.74</b>
4	1000	-1.47	<b>-1.46</b>	-1.76	<b>-1.72</b>
4	2500	<b>-1.43</b>	-1.44	-1.68	<b>-1.67</b>
8	100	-1.74	<b>-1.66</b>	-2.18	<b>-2.07</b>
8	500	-1.66	<b>-1.63</b>	-2.02	<b>-1.92</b>
8	1000	<b>-1.55</b>	-1.58	-1.95	<b>-1.91</b>
8	2500	<b>-1.48</b>	-1.53	-1.88	<b>-1.87</b>
20	100	-2.04	<b>-2.02</b>	-2.59	<b>-2.31</b>
20	500	<b>-1.94</b>	-1.99	-2.41	<b>-2.28</b>
20	1000	<b>-1.81</b>	-1.94	-2.31	<b>-2.27</b>
20	2500	<b>-1.66</b>	-1.84	<b>-2.27</b>	-2.32

Table 1: Results of simulation study

Figure 5 gives some further intuition as to how functional BART performs across several values of  $x_i$  in the  $P = 4$  case: on a held-out sample, it tends to smooth out the bumps in  $f(t; x)$  much less than ordinary BART. We conclude that functional BART has consistently superior out-of-sample performance, with the most significant gains in scenarios with small sample sizes and higher dimensions. Functional BART performs especially well compared to BART when these factors are combined.

## 5 Nonparametric functional regression for stillbirth risk

We now turn to our motivating example, an analysis of pregnancy-outcomes data using functional BART.

### 5.1 Background

Determining the optimal gestational age for delivery of a pregnancy has long posed challenges for obstetricians, who carefully consider the optimal gestational age for delivery with the aim to minimize risk of adverse outcomes to both mother and infant. An especially serious fetal outcome is stillbirth, defined as death in utero after 20 weeks' gestation.

Stillbirth is a significant public health concern which affects tens of thousands of Americans each year. In the U.S. in 2013, the stillbirth rate was 5.96 fetal deaths per 1,000 live births (MacDorman and Gregory, 2015). The National Vital Statistics System (NVSS) notes that stillbirth has been significantly overlooked in public-health research and practical obstetrics guidance, and its mechanisms are not thoroughly understood. We might recommend early delivery to avoid stillbirth, but this course of action has serious consequences. Both preterm and early term births are associated with increased risk of neonatal mortality and morbidity. Several studies have reported a relationship between neuro-developmental and cognitive outcomes and gestational age at delivery in late preterm and early term births. Besides health outcomes, there are also financial costs of care for these infants (e.g. Muraskas and Parsi, 2008; Kornhauser and Schneiderman, 2010).

Obstetricians benefit greatly from access to estimates of stillbirth risk functions over gestational age. Accurate stillbirth risk information informs clinical practice, and obstetricians can manage a patient accordingly if the risk of stillbirth increases at earlier gestational ages than typical, is generally higher, or increases more drastically as pregnancy progresses. Obstetricians may manage the pregnancy by inducing labor earlier, increasing frequency of supervision, or recommending smoking cessation or diet modifications, to name a few among many possible courses of action. Uncertainty quantification also plays an important role; intuitively, practitioners are most comfortable managing the types of cases they see repeatedly. Providing estimated risk curves for individual patients which include uncertainty estimation gives evidence-based guidance for understanding which cases are less clear-cut.

Previous research has focused more heavily on researching neonatal death, at the expense of understanding stillbirth (e.g. Bailit et al., 2010; Clark et al., 2010; U. et al., 2011). A more recent line of work attempts to refine previous broad conclusions by seeking to model stillbirth risk based on a patient's individual risk factors. In particular, Mandujano

et al. (2013) model risk curves for patients stratified into two broad categories: low risk versus high risk. Here “high risk” is determined by presence or absence of at least one of several preexisting maternal conditions (e.g. diabetes or chronic hypertension). The model provides two stillbirth risk curves, one each for the high-risk and low-risk groups, for a U.S. cohort.

Clinically speaking, this approach has several shortcomings. It collapses many medical conditions with distinct etiologies into a single “high risk” category. It focuses only on the mother’s medical condition, ignoring known risk factors for adverse pregnancy outcomes, such as the mother’s race/ethnicity, age, parity, and weight gain, among others. It ignores fetal covariates such as sex and birth weight (estimated by ultrasound). It does not allow for the possibility of statistical interactions between risk factors.

There is growing recognition of the benefits of data-driven analysis in healthcare, which requires careful specification of a statistical model. Clinical intuition supports smoothly evolving risk curves over the progression of a pregnancy; the key statistical point is that risk of stillbirth evolves smoothly over time, and changes as a function of the maternal-fetal risk factors. Knowledge of the risk function for each pregnancy would inform obstetricians’ treatments of their patients.

Suppose that  $x$  represents a vector of covariates for a particular maternal-fetal dyad (including maternal risk factors, such as diabetes, hypertension, and sociodemographic variables; and fetal characteristics, such as sex or ultrasound-estimated fetal weight). Now let  $t$  represent gestational age (discrete time, measured in weeks or days). Our object of statistical interest is the hazard function for stillbirth,  $h(t; x)$ , which represents the conditional probability of stillbirth at gestational age  $t$ , given that a fetus has survived in utero through gestational age  $t - 1$ . This risk function is not well understood, and we expect that it changes, in complicated nonlinear ways with maternal-fetal covariates  $x$ . To estimate it, we need a large data set, since the outcomes are relatively rare—but we also need a scalable statistical model for functional regression that is capable of handling nonlin-

earities and multi-way interactions of unknown form, and that can also generate sensible error bars. Specifically, we use functional BART to model the risk curve for stillbirth over the range of viable gestational ages. We find that patients with different combinations of characteristics have different risk curves, with some patients' risk of stillbirth rising more rapidly and earlier in pregnancy. We also find that patients with more complex combinations of maternal-fetal characteristics, such as a patient who is both diabetic and older and has a low birth weight, have more uncertainty in their estimated risk curves. These findings support the importance of personalizing estimation of stillbirth risk for each patient.

## 5.2 Data preprocessing

Our analysis uses anonymized electronic health record data from the National Center for Health Statistics. Each medical record consists of a pregnancy, with several variables constructed from available fields. Analysis is limited to complete cases consisting of pregnancies delivered from 34 to 42 weeks, as this the range of plausible viability where clinicians may opt to induce a pregnancy based on information from one of the risk curves. Pregnancy would not be induced before 34 weeks regardless of risk curve projections barring exceptional circumstances. Pregnancies were classified by outcome as stillbirth, neonatal death, or live birth with neither adverse outcome.

Maternal age was discretized into 5-year age groups:  $leq20$ , 20-24, 25-29, 30-34, etc. with women over 45 grouped together due to small sample sizes. Maternal ethnicities were categorized as White Non-Hispanic, Black Non-Hispanic, Hispanic, and Other. Maternal weight gain and fetal birth weight were discretized into quantile groups  $([0, 0.1], [0.1, 0.25], [.25, 0.75], [0.75, 0.90], \text{ and } [0.90, 1.0])$ .

Maternal covariates include the presence of diabetes mellitus, chronic hypertension, and "other" risk factors. We classify pregnancies as having other risk factors based on the presence of: anemia, cardiac disease, hemoglobinopathy, lung disease, Rh sensitization,

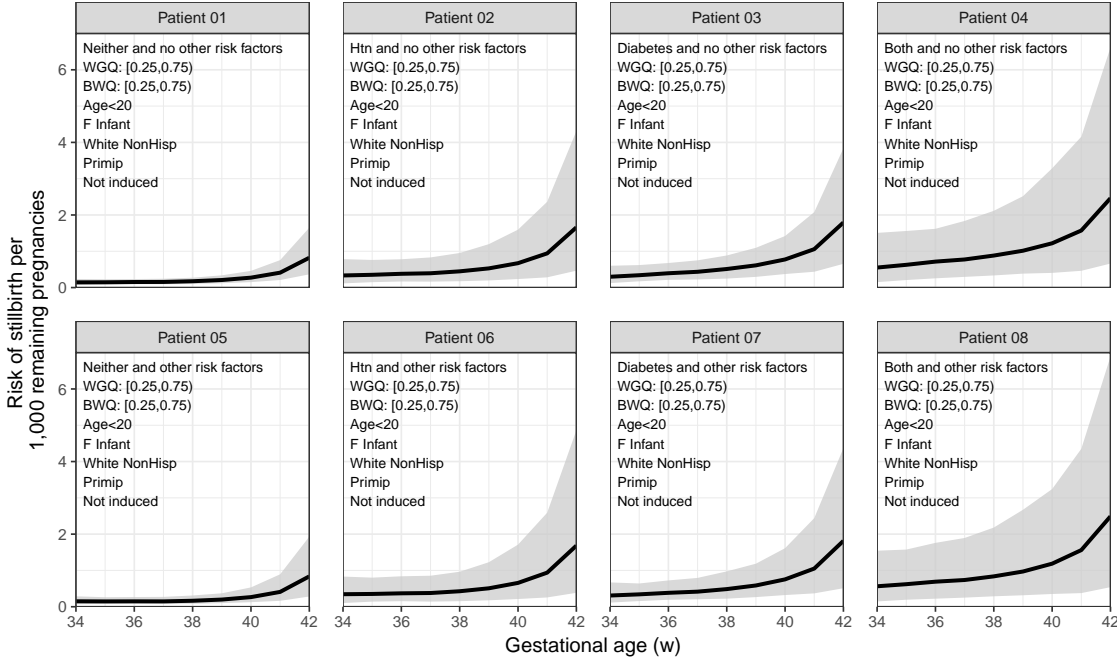


Figure 7: Stillbirth risk for diabetic and hypertensive patients: without other risk factors, with other risk factors, with induced labor, and with induced labor and other risk factors

and renal disease. Pregnancy-related complications such as gestational diabetes, abruption, and preeclampsia were excluded.

### 5.3 Analysis and results

We use the subscript  $i$  to denote a pregnancy observed at a specific gestational age  $t_i$ . Let  $y_i$  be an indicator of whether stillbirth has occurred at each gestational age; each pregnancy is present in the data set for all times prior to and including the event, i.e. birth, to induce correct conditional probabilities as we are effectively modeling a discrete-time hazard function. Let  $t_i \in \{34, 35, \dots, 42\}$  consist of nine evenly-spaced weeks. We define  $x_i$  as the vector of maternal-fetal covariates for each patient, including maternal age group (in 5-year bins, with  $< 20$  and  $45+$  forming their own groups), parity, ethnicity, infant sex, presence of diabetes and/or hypertension, presence of other risk factors, parity, whether the pregnancy was induced, and birth weight and weight gain during pregnancy quantiles.

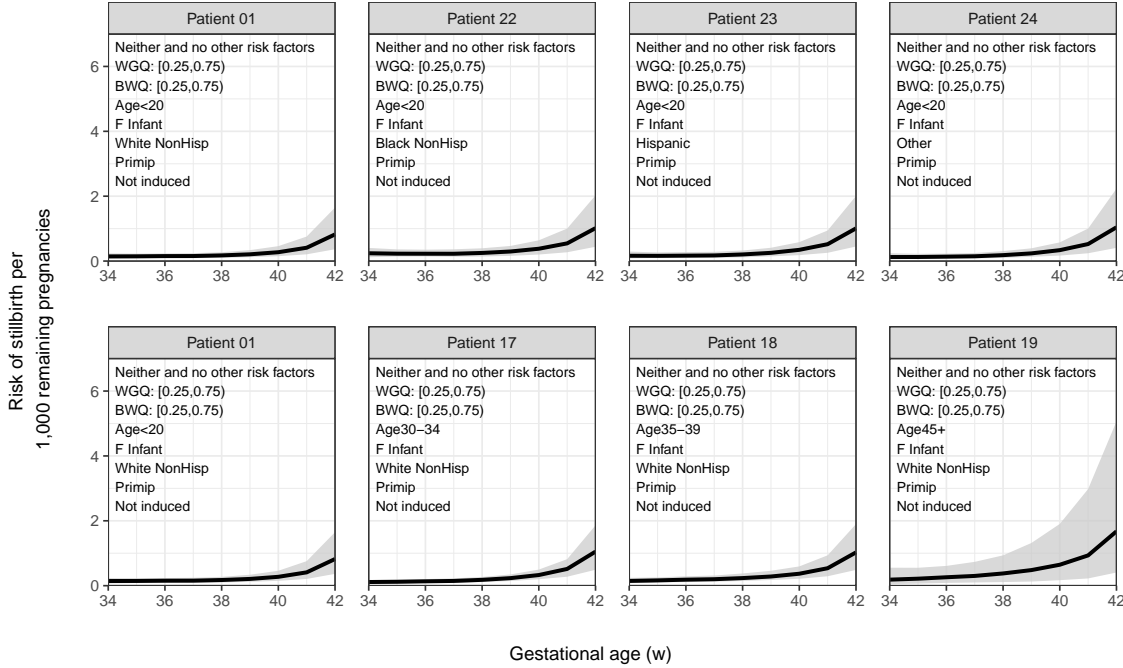


Figure 8: Stillbirth risk for patients of varying ethnicities and ages

Other risk factors included: anemia, cardiac disease, lung disease, diabetes mellitus, hemoglobinopathy, chronic hypertension, rental disease, or Rh sensitization. Pregnancies without any of these conditions were not considered to have other risk factors, and pregnancy-related complications, such as gestational diabetes, abruption, or preeclampsia, were not included as risk factors.

Birth weight and weight gain quantiles were divided into the following categories: [0,0.10), [0.10,0.25), [0.25,0.75), [0.75,0.90), [0.90,1). Weight gain is measured over the course of the pregnancy until delivery. Birth weight is a proxy for fetal weight in utero, which is difficult to measure, and highly variable.

We use the natural extension of the BART probit formulation to model the risk of a stillbirth at time  $t$  given survival in utero up to time  $t$ , per 1,000 pregnancies. For our selection of hyperparameters, we tuned the expected number of crossings, arriving at 1.5 using the method described in the Appendix. We set hyperparameters  $(\nu, \lambda)$  as recommended in Chipman et al. (2010). Data is selected using case-control sampling, stratified on combinations of patient characteristics, gestational age, and stillbirth status. Predic-

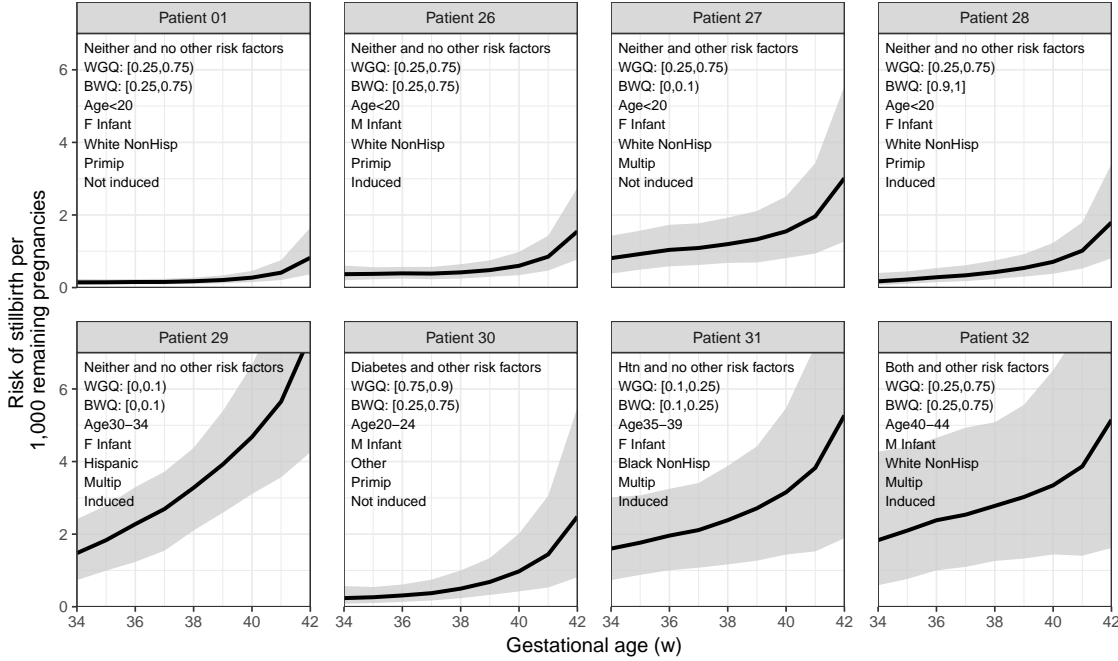


Figure 9: Stillbirth risk for patients with combinations of maternal-fetal characteristics

tions are made for a selection of hypothetical patients, representing various configurations of maternal-fetal characteristics.

The baseline patient for these comparisons is a young (< 20), white, primiparous patient, giving birth to a female infant, without hypertension, diabetes, or other risk factors. Labor is not induced, and both birth weight and weight gain during pregnancy are in their respective middle quantile groups [0.25-0.75].

Clinical knowledge intuits that diabetes and hypertension will likely be significant drivers of increased risk of stillbirth. Panel 7 compares the baseline patient to patients with the same characteristics, but with the introduction of hypertension, then diabetes, followed by both hypertension and diabetes. The first row of this panel confirms our clinical intuition; the risk of stillbirth increases as pregnancy progresses. (All stillbirth could be prevented by inducing early enough, at the expense of survival after delivery; extended time in utero increases risk.) Moreover, the level of risk varies based on introduction of diabetes and/or hypertension, with the combination having the greatest increase in stillbirth risk. We see a corresponding increase in uncertainty as we introduce

hypertension, then diabetes, then both.

In the second row of Panel 7, we add other risk factors to the diabetes-hypertension combinations; addition of other risk factors does not significantly change the risk curves. This suggests that risk differences in the two-group approach (Mandujano et al., 2013) are largely driven by diabetes and hypertension, with little contribution from other diseases.

Panel 8 compares the baseline patient to patients with the same characteristics, but varying ethnicities and ages. The risk curve differences for ethnicity are negligible; we find disease status for hypertension and diabetes to be a much stronger driver for increased stillbirth risk. The second row of the panel confirms clinical knowledge that pregnancy is riskier as age increases, with individuals in the 45+ age group at the highest risk of all age demographics.

Panel 9 compares the baseline patient to patients with varying combinations of risk factors. Risk curves vary markedly by combination of maternal-fetal characteristics, as does level of uncertainty. We note the posterior credible intervals are much wider for patients with complex combinations of characteristics. A common theme in these panels is an increase in uncertainty in cases that are seen less frequently, mirroring an obstetrician who sees many similar patients and so is less certain of treatment for an outlier.

## 6 Final remarks

Our functional BART model is a novel extension of BART for functional response regression problems. Our results show that functional BART removes many of the researcher degrees of freedom associated with the functional linear model, especially in the presence of interactions and nonlinear effects. FunBART has excellent predictive performance, and it consistently outperforms ordinary BART in settings with a smooth functional response, especially in scenarios with higher dimension and/or smaller sample sizes. Hyperparameters are set efficiently via data-driven approaches using recommendations from Chip-

man et al. (2010) and our suggested method for tuning the length-scale of the covariance function. Functional BART provides regularization in the form of constraining trees to be shallow learners in the prior, which is a well studied and highly successful approach to regularization in ordinary scalar regression.

We have not benchmarked our method against joint models that attempt to estimate a full response surface for the outcome  $y$  in both  $x$  and  $t$  jointly. (Gaussian processes would be a canonical example of such a model.) These methods tend to scale poorly in both the sample size  $n$  (often  $n^3$ ) and the dimensionality of the predictor space  $p$  (usually exponentially). Joint methods also require a choice of metric in for measuring distances between points in  $(x, t)$  space jointly. This introduces many extra researchers degrees of freedom, especially if  $x$  involves binary or categorical covariates; it is also highly dependent on any transformations of numerical variables in  $x$ , e.g. to a log space. For these reasons, full joint models are rarely practical in most functional regression problems. Functional BART, on the other hand, handles categorical predictors seamlessly, is invariant to transformations of the predictors, and avoids the curse of dimensionality by shrinking towards additivity.

The stillbirth risk analysis we have conducted represents a substantial advancement on previous work in obstetrics (Mandujano et al., 2013). We provide evidence that simply categorizing patients into low-risk and high-risk groups based on presence or absence of a list of disease conditions is insufficient for accurately describing the risk of stillbirth at various gestational ages. As demonstrated in Panel 9, maternal-fetal covariates such as age, weight gain, and birth weight play a significant role in risk of stillbirth. The sheer variety of these risk curves for different combinations of predictors show that the data exhibit rich and complex interactions that would be exceedingly difficult to capture using a functional linear model. Moreover, our fully Bayesian approach naturally allow clinicians to quantify uncertainty about stillbirth risk, which appropriately varies from patient to patient.

There are some limitations in our analysis of stillbirth risk. One potential limitation

of our work is use of weight gain quantile. For example, slow weight gain may cause an increased risk of stillbirth. Yet causality can also run in the other direction: that is, weight gain may level off due to fetal death in utero. However, we do not believe potential reverse causality in weight gain is driving our findings; effect of differences in weight gain alone is modest.

Future areas of methodological work may include extension of functional BART to a causal inference framework for application to observational data, as well as extension to other priors with other types of structure. Also, partial dependence plots may be used to assess effect of individual covariates, but quantifying more complex features like interactions and linearities from the functional BART fit is an area of future work, same as in the BART model.

## Supplementary materials

The supplementary materials include the R scripts that were used for the study, which can be found at <https://github.com/jestarling/functionalbart/>. The Functional BART R package **funbart** can be found at <https://github.com/jestarling/funbart/>.

## Appendix

Here we provide additional detail regarding tuning the expected number of crossings  $E[N_T(0)]$  for calculating the covariance's length-scale parameter.

We select the optimal  $E[N_T(0)]$  by beginning with a grid of candidate values  $e_c \in \{e_1, \dots, e_C\}$ . For each  $e_c$  value, we fit the functional BART model and calculate WAIC (Watanabe, 2013), yielding a grid of WAIC values  $\Omega = \{\omega_1, \dots, \omega_C\}$ .

The WAIC values contain Monte Carlos variation; to overcome this, we fit a cubic spline model to  $\Omega$ . Let  $\zeta$  be the standard deviation of the residuals from this model fit.

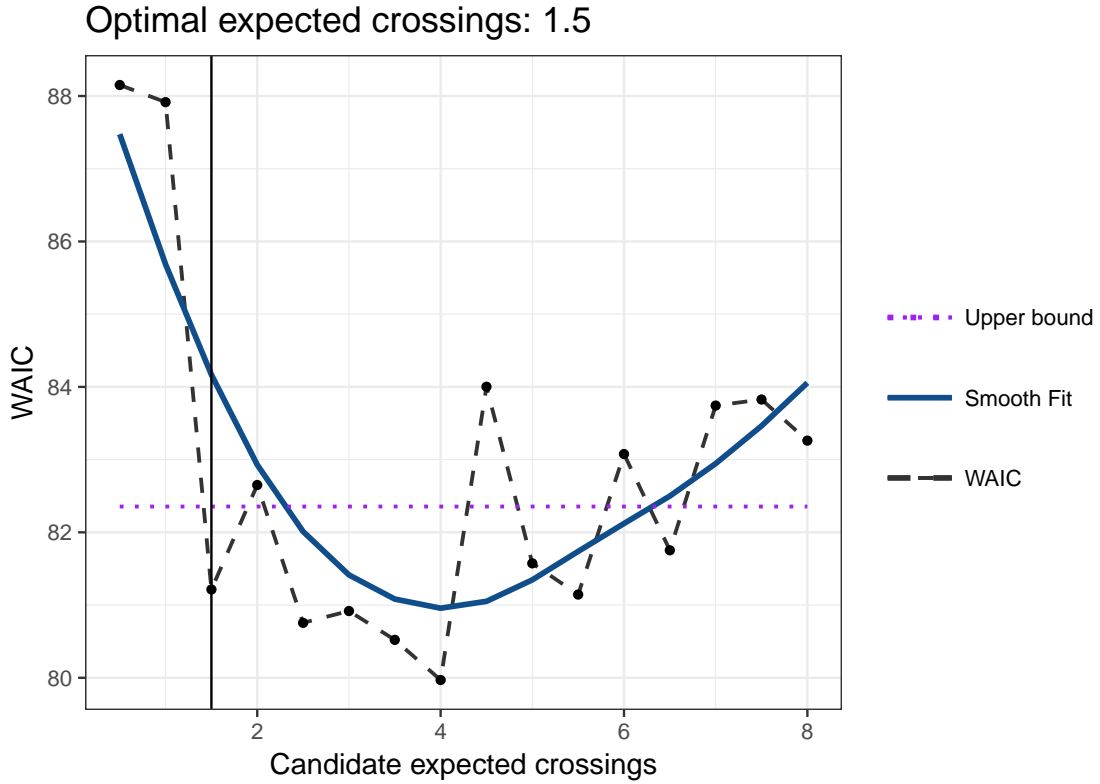


Figure 10: Example of expected crossings tuning

We select the smallest number of expected crossings  $e_c$  where the corresponding  $\omega_c$  is within one standard deviation of  $\min(\Omega)$ . This approach encourages smoothing while maintaining performance. Figure 10 gives an example of this tuning for the toy example from Section 2.3.

Other methods such as cross-validation could easily be used for tuning the expected number of crossings; we find this data-driven approach to be efficient while still yielding good results.

## REFERENCES

J. H. Albert and S. Chib. Bayesian analysis of binary and polychotomous response data. *Journal of the American Statistical Association*, 88(422):669–679, 1993.

J. Bailit, K. Gregory, and U. Reddy. Maternal and neonatal outcomes by labor onset type and gestational age. *Am J Obstet Gynecol*, 202:245.e1-12, 2010.

J. Bleich, A. Kapelner, E. I. George, and S. T. Jensen. Variable selection for bart: An application to gene regulation. *The Annals of Applied Statistics*, 8(3):1750–1781, 2014.

H. A. Chipman and R. E. McCulloch. R package ‘bayestree’, 2016. URL <https://CRAN.R-project.org/package=BayesTree>.

H. A. Chipman, E. I. George, and R. E. McCulloch. Bayesian cart model search. *Journal of the American Statistical Association*, 93(443):935–948, 1998.

H. A. Chipman, E. I. George, and R. E. McCulloch. Bart: Bayesian additive regression trees. *The Annals of Applied Statistics*, 4(1):266–298, 03 2010.

S. Clark, D. Frye, and J. Myers. Reduction in elective delivery at  $\leq 39$  weeks of gestation: comparative effectiveness of 3 approaches to change and the impact on neonatal intensive care admission and stillbirth. *Am J Obstet Gynecol*, 203:449.e1-6, 2010.

P. H. C. Eilers and B. D. Marx. Flexible smoothing with b-splines and penalties. *Statistical Science*, 11(2):89–121, 05 1996.

A. Gelman. Prior distributions for variance parameters in hierarchical models (comment on article by browne and draper). *Bayesian Analysis*, 1(3):515–534, 09 2006.

R. Gramacy and H. K. Lee. Bayesian treed Gaussian process models with an application to computer modeling. *Journal of the American Statistical Association*, 103(483):1119–30, 2008.

P. R. Hahn, J. S. Murray, and C. M. Carvalho. Bayesian regression tree models for causal inference: regularization, confounding, and heterogeneous effects. *arXiv:1706.09523*, 2017.

B. Hernández, A. Raftery, and S. e. a. Pennington. Bayesian additive regression trees using bayesian model averaging. *Stat Comput*, 28:869, 2018.

J. L. Hill. Bayesian nonparametric modeling for causal inference. *Journal of Computational and Graphical Statistics*, 20(1):217–240, 2011.

A. Kapelner and J. Bleich. bartmachine: Machine learning with bayesian additive regression trees. Available at *arXiv:1312.2171*, 2014.

M. Kornhauser and R. Schneiderman. How plans can improve outcomes and cut costs for preterm infant care. *Managed Care*, 2010.

M. F. Kratz. Level crossings and other level functionals of stationary gaussian processes. *Probability Surveys*, 3:230–288, 2006.

B. Lakshminarayanan, D. Roy, and Y. Teh. Particle gibbs for bayesian additive regression trees. *Artificial Intelligence and Statistics*, 2015.

A. Linero and Y. Yang. Bayesian regression tree ensembles that adapt to smoothness and sparsity. *arXiv:1707.09461v1 [stat.ME]*, 2017.

A. R. Linero. Bayesian regression trees for high-dimensional prediction and variable selection. *Journal of the American Statistical Association*, 0(0):1–11, 2018.

M. F. MacDorman and E. C. Gregory. Fetal and perinatal mortality: United states, 2013. *National Vital Statistics Report; NVSS*, 66, No. 6, 2015.

A. Mandujano, T. Waters, and S. Myers. The risk of fetal death: current concepts of best gestational age for delivery. *Am J Obstet Gynecol*, 208(207), 2013.

R. E. McCulloch, R. Sparapani, R. Gramacy, and et al. Package ‘bart’, 2018. URL <https://CRAN.R-project.org/package=BART>.

J. S. Morris. Functional regression. *arXiv:1406.4068 [stat.ME]*, 2014.

J. Muraskas and K. Parsi. The cost of saving the tiniest lives: Nicus versus prevention. *AMA Journal of Ethics, Virtual Mentor*, 2008.

M. T. Pratola, H. A. Chipman, J. R. Gattiker, D. M. Higdon, R. McCulloch, and W. N. Rust. Parallel bayesian additive regression trees. *Journal of computational and graphical statistics: a joint publication of American Statistical Association, Institute of Mathematical Statistics, Interface Foundation of North America*, 23(3):830–852, 2014. ISSN 1061-8600.

J. Ramsay. *Functional Data Analysis*. New York ; Berlin : Springer, 1997.

J. Q. Shi, B. Wang, R. MurraySmith, and D. M. Titterington. Gaussian process functional regression modeling for batch data. *Biometrics*, 63(3):714–723, 2007.

Sparapani, Logan, MucCulloch, and Laud. Nonparametric survival analysis using bayesian additive regression trees (bart). *Statistics in Medicine*, 35(16):2741–2753, 2016.

R. U., B. V.R., D. T., and et. al. Term pregnancy: a period of heterogeneous risk for infant mortality. *Obstet Gynecol*, 117:1279-87, 2011.

S. Watanabe. A widely applicable bayesian information criterion. *Journal of Machine Learning Research*, 14:867–897, 2013.

J. Xu, S. L. Murphy, K. D. Kochanek, and B. A. Bastian. Deaths: Final data for 2013. *National Vital Statistics Report; NVSS*, 64(2), 2013.